Citation: Kandala SS, Uchida TK, Vyasarayani CP. Pole placement for time-delayed systems using Galerkin approximations. Journal of Dynamic Systems, Measurement, and Control 141(5): 051012, 2019. doi: 10.1115/1.4042465.

Pole placement for time-delayed systems using Galerkin approximations

Shanti S. Kandala[a], Thomas K. Uchida[b], C.P. Vyasarayani[a,*]

[a] Department of Mechanical and Aerospace Engineering, Indian Institute of Technology Hyderabad

Kandi, Sangareddy 502285, Telangana, India

[b] Department of Bioengineering, Stanford University

James H. Clark Center, 318 Campus Drive, Stanford, California 94305, U.S.A.

[*] Address all correspondence to this author. E-mail address: vcprakash@iith.ac.in

Abstract

Many dynamic systems of practical interest have inherent time delays and thus are governed by delay differential equations (DDEs). Because DDEs are infinite dimensional, time-delayed systems may be difficult to stabilize using traditional controller design strategies. We apply the Galerkin approximation method using a new pseudoinverse-based technique for embedding the boundary conditions, which results in a simpler mathematical derivation than has been presented previously. We then use the pole placement technique to design closed-loop feedback gains that stabilize time-delayed systems, and verify our results through comparison to those reported in the literature. Finally, we perform experimental validation by applying our method to stabilize a rotary inverted pendulum system with inherent sensing delays as well as additional time delays that are introduced deliberately. The proposed approach is easily implemented and performs at least as well as existing methods.

1 Introduction

Many dynamic processes can be aptly described as time-delayed systems, in which time derivatives of the state variables are explicit functions of past states. For example, time-delayed systems are encountered in the modeling of control systems [1] (e.g., due to sensing and actuation delays), machining processes [2], and lasers [3]. If all delays are negligible, the mathematical model of such a system can be reduced to ordinary differential equations (ODEs). For a system governed by ODEs to be stable, all characteristic roots must lie in the left half of the complex plane. An inherently unstable system can be stabilized using the *pole placement* technique, whereby a closed-loop controller is designed such that the poles of the controlled system lie in the left half of the complex plane. Pole placement for systems of ODEs has been widely studied in the literature [4].

In the presence of non-negligible delays, the equations governing the dynamics of a time-delayed system are delay differential equations (DDEs). As is the case with ODEs, systems of DDEs can be stabilized by placing the poles of the controlled system in the left half of the complex plane. Unlike an ODE, however, the characteristic equation of a DDE is a quasi-polynomial with infinitely many roots. Although the stability of a DDE is dominated by its rightmost eigenvalue in the complex plane, its infinite dimensionality can make the pole placement problem challenging [5–7].

A system governed by DDEs can be stabilized by adjusting system parameters and/or tuning delays [8–10], using optimization-based [11–13] and non-optimization-based [14] strategies. Michiels et al. [11] proposed a continuous pole placement technique using the gradient sampling algorithm [15], which was among the first attempts at applying an eigenvalue optimization approach to infinite-dimensional systems. Optimization strategies were also used by Vanbiervliet et al. [16]

for stabilizing time-delayed systems by tuning system parameters, and by Vyhlídal et al. [13] for stabilizing time-delayed systems using state-derivative feedback controllers. Yi et al. [7, 17] solved the eigenvalue assignment problem using the Lambert W function, which allows one to write the analytical expressions in terms of the system parameters, similar to the state-transition matrix in linear ODE systems. The method of Yi et al. was limited to systems comprising a single discrete delay; Wei et al. [18] extended the Lambert W function to handle distributed delays. Niu et al. [14] proposed an eigenvalue assignment technique based on the generalized Runge–Kutta method, but applied their method to DDEs with only a single delay.

Several methods have been used in the literature for finding the characteristic roots of DDEs. Examples include the Lambert W function [6, 19–21], Galerkin approximations [22–24], Laplace transforms [25], semi-discretization [26], spectral tau methods [27], pseudospectral collocation [28–30], time finite elements [31,32], continuous-time approximation [33,34], and finite-difference methods [35, 36]. In the present work, we obtain the characteristic roots of DDEs using the Galerkin approximation method, in which the DDE is first converted into a partial differential equation (PDE) with boundary conditions; the PDE is then approximated by a system of ODEs. The eigenvalues of the resulting ODE system approximate the characteristic roots of the original DDE. The efficacy of the Galerkin approximation method has already been established for studying the stability of DDEs with constant coefficients [37], time-periodic coefficients [38], time-periodic delays [39], and distributed delays [24]. In all previous work, the present authors have handled the boundary conditions within the Galerkin framework using the spectral tau and Lagrange multiplier methods. In the present work, we propose a new pseudoinverse-based strategy for embedding the boundary conditions into the Galerkin approximation, which simplifies the derivation of the final

system of ODEs. We then apply an optimization strategy to solve the pole placement problem.

The paper is organized as follows. In Section 2, we describe the optimization problem and mathematical modeling. In Section 3, we verify our approach through comparison to results reported in the literature using existing methods. We then further validate our approach in Section 4 by stabilizing DDEs obtained from the literature [11, 14]. In Section 5, we use our approach to stabilize an experimental apparatus with inherent sensing delays as well as additional time delays that are introduced deliberately. Finally, conclusions are provided in Section 6.

2 Pole Placement for Delay Differential Equations

A system's closed-loop pole locations determine its stability characteristics as well as the characteristics of its time response, such as its rise time and settling time. The pole placement technique can be used to adjust the closed-loop pole locations for stabilizing both single-input single-output (SISO) and multiple-input multiple-output (MIMO) systems.

2.1 Problem definition

Consider the following system of DDEs, expressed here in state-space form:

$$\dot{\mathbf{x}}(t) + \mathbf{A}\mathbf{x}(t) + \sum_{q=1}^{m} \mathbf{B}_q u_q(t-\tau_q) = \mathbf{0} \tag{1a}$$

$$u_q(t-\tau_q) = \mathbf{K}_q^{\mathrm{T}} \mathbf{x}(t-\tau_q), \quad q = 1, 2, \ldots, m \tag{1b}$$

where $\mathbf{x}(t) \triangleq [x_1(t), x_2(t), \ldots, x_P(t)]^{\mathrm{T}}$ is the state vector, $\mathbf{u}(t) \triangleq [u_1(t), u_2(t), \ldots, u_m(t)]^{\mathrm{T}}$ is the control vector, $\mathbf{A} \in \mathbb{R}^{P \times P}$, $\mathbf{B}_q \in \mathbb{R}^{P \times 1}$, $\mathbf{K}_q \in \mathbb{R}^{P \times 1}$, and delays $\tau_q > 0$. Given $\mathbf{A}$, $\mathbf{B}_q$, and delays τ_q, the objective is to determine the feedback gains $\mathbf{K}_q$ that are necessary to stabilize the

system (i.e., to move all poles into the left half of the complex plane). We optimize gains $\mathbf{K}_q$ by minimizing the following objective function:

$$J = \Big(\mathrm{Re}\left(\lambda_{\max}\left(\mathbf{K}_q\right)\right) + \alpha \Big)^2 \tag{2}$$

where $\mathrm{Re}\left(\lambda_{\max}\right)$ is the real part of the rightmost eigenvalue, which is a function of feedback gains $\mathbf{K}_q$, and $\alpha > 0$ is a parameter specifying the desired distance between $\lambda_{\max}$ and the imaginary axis. In this work, Eq. (2) is first solved with $\alpha = \alpha_0$ where $\alpha_0 > 0$ (i.e., all poles are placed in the left half of the complex plane). We then increase α by $\delta\alpha$ and solve Eq. (2) again, repeating this process until the optimal objective function value $J > 0$ (i.e., until $\mathbf{K}_q$ cannot be found to move $\lambda_{\max}$ to the location specified by α). We use $\alpha_0 = \delta\alpha = 1$ in the examples below. This simple algorithm was sufficient for our purposes; however, a more complex optimization problem could be designed to include other considerations, such as hardware limitations (e.g., by introducing constraints) or a desired time-delay stability margin.

2.2 Mathematical modeling

In this section, we extend the work of Vyasarayani, Sadath, and colleagues [23,24,37] and develop a new pseudoinverse-based Galerkin approximation method for finding the characteristic roots of DDEs. We begin by considering the following system of DDEs:

$$\dot{\mathbf{x}}(t) + \mathbf{A}\mathbf{x}(t) + \sum_{q=1}^{m} \mathbf{B}_q \mathbf{K}_q^{\mathrm{T}} \mathbf{x}(t - \tau_q) = \mathbf{0} \tag{3}$$

where $\mathbf{x}(t)$, $\mathbf{A}$, $\mathbf{B}_q$, $\mathbf{K}_q$, and τ_q are as defined above. The characteristic equation of Eq. (3) is obtained by substituting $\mathbf{x}(t) = \mathbf{x}_0 e^{st}$, the determinant of which we equate to zero:

$$\det\left(s\mathbf{I} + \mathbf{A} + \sum_{q=1}^{m} \mathbf{B}_q \mathbf{K}_q^{\mathrm{T}} e^{-s\tau_q} \right) = 0 \tag{4}$$

Equation (4) is a quasi-polynomial due to the presence of transcendental terms $e^{-s\tau_q}$ and, hence, has infinitely many roots. The roots of Eq. (4) can be computed by formulating an abstract Cauchy problem, whereupon we obtain and solve a large linear eigenvalue problem.

We begin by converting the system of DDEs (Eq. (3)) into a system of PDEs with time-dependent boundary conditions. We introduce the following transformation:

$$\mathbf{y}(s,t) = \mathbf{x}(t+s) \tag{5}$$

where $\mathbf{y}$ is a function of $s \in [-\tau, 0]$ and t, with $\tau \triangleq \max(\tau_1, \tau_2, \ldots, \tau_m)$. An abstract Cauchy problem is obtained by differentiating Eq. (5) with respect to s and t:

$$\frac{\partial \mathbf{y}(s,t)}{\partial t} = \frac{\partial \mathbf{x}(t+s)}{\partial (t+s)} \frac{\partial (t+s)}{\partial t} \quad \Rightarrow \quad \frac{\partial \mathbf{y}(s,t)}{\partial t} = \frac{\partial \mathbf{x}(t+s)}{\partial (t+s)} \tag{6a}$$

$$\frac{\partial \mathbf{y}(s,t)}{\partial s} = \frac{\partial \mathbf{x}(t+s)}{\partial (t+s)} \frac{\partial (t+s)}{\partial s} \quad \Rightarrow \quad \frac{\partial \mathbf{y}(s,t)}{\partial s} = \frac{\partial \mathbf{x}(t+s)}{\partial (t+s)} \tag{6b}$$

Upon equating Eqs. (6a) and (6b), we obtain the following PDE:

$$\frac{\partial \mathbf{y}(s,t)}{\partial t} = \frac{\partial \mathbf{y}(s,t)}{\partial s}, \quad s \in [-\tau, 0] \tag{7}$$

The boundary conditions for Eq. (7) are computed by substituting $s = 0$ and $s = -\tau$ into Eq. (5):

$$\mathbf{y}(0,t) = \mathbf{x}(t) \quad \Rightarrow \quad \left.\frac{\partial \mathbf{y}(s,t)}{\partial t}\right|_{s=0} = \dot{\mathbf{x}}(t) \tag{8a}$$

$$\mathbf{y}(-\tau, t) = \mathbf{x}(t-\tau) \tag{8b}$$

and then combining these relations with Eq. (3):

$$\left.\frac{\partial \mathbf{y}(s,t)}{\partial t}\right|_{s=0} + \mathbf{A}\mathbf{y}(0,t) + \sum_{q=1}^{m} \mathbf{B}_q \mathbf{K}_q^{\mathrm{T}} \mathbf{y}(-\tau_q, t) = \mathbf{0} \tag{9}$$

We now assume a series solution for the PDE (Eq. (7)):

$$y_i(s,t) = \sum_{j=1}^{\infty} \phi_{ij}(s) \eta_{ij}(t), \quad i = 1, 2, \ldots, P \tag{10}$$

where $\phi_{ij}(s)$ are the basis functions, $\eta_{ij}(t)$ are the time-dependent coordinates, i represents the index into the state vector $\mathbf{x}(t)$, and j represents the corresponding term in each basis function. Because it is impossible to consider the entire infinite series, we truncate the series at N terms:

$$y_i(s,t) \approx \boldsymbol{\phi}_i^{\mathrm{T}}(s)\boldsymbol{\eta}_i(t), \quad i = 1, 2, \ldots, P \tag{11}$$

where $\boldsymbol{\phi}_i(s) \triangleq [\phi_{i1}(s), \phi_{i2}(s), \ldots, \phi_{iN}(s)]^{\mathrm{T}}$ and $\boldsymbol{\eta}_i(t) = [\eta_{i1}(t), \eta_{i2}(t), \ldots, \eta_{iN}(t)]^{\mathrm{T}}$. We define matrix $\boldsymbol{\Psi}(s) \in \mathbb{R}^{NP \times P}$ and vector $\boldsymbol{\beta}(t) \in \mathbb{R}^{NP \times 1}$ as follows:

$$\boldsymbol{\Psi}(s) = \begin{bmatrix} \boldsymbol{\phi}_1(s) & \mathbf{0} & \cdots & \mathbf{0} \\ \mathbf{0} & \boldsymbol{\phi}_2(s) & \cdots & \mathbf{0} \\ \vdots & \vdots & \ddots & \vdots \\ \mathbf{0} & \mathbf{0} & \cdots & \boldsymbol{\phi}_P(s) \end{bmatrix} \tag{12a}$$

$$\boldsymbol{\beta}(t) = \left[\boldsymbol{\eta}_1^{\mathrm{T}}(t), \boldsymbol{\eta}_2^{\mathrm{T}}(t), \ldots, \boldsymbol{\eta}_P^{\mathrm{T}}(t)\right]^{\mathrm{T}} \tag{12b}$$

whereupon we can express Eq. (11) in vector form:

$$\begin{aligned} \mathbf{y}(s,t) &= \left[\boldsymbol{\phi}_1^{\mathrm{T}}(s)\boldsymbol{\eta}_1(t), \boldsymbol{\phi}_2^{\mathrm{T}}(s)\boldsymbol{\eta}_2(t), \ldots, \boldsymbol{\phi}_P^{\mathrm{T}}(s)\boldsymbol{\eta}_P(t)\right]^{\mathrm{T}} \\ &= \boldsymbol{\Psi}^{\mathrm{T}}(s)\boldsymbol{\beta}(t) \end{aligned} \tag{13}$$

Next, we substitute the series solution (Eq. (13)) into the original PDE (Eq. (7)):

$$\boldsymbol{\Psi}^{\mathrm{T}}(s)\dot{\boldsymbol{\beta}}(t) = \boldsymbol{\Psi}'(s)^{\mathrm{T}}\boldsymbol{\beta}(t) \tag{14}$$

where $\boldsymbol{\Psi}'(s)$ denotes the derivative of $\boldsymbol{\Psi}(s)$ with respect to s. Pre-multiplying Eq. (14) by $\boldsymbol{\Psi}(s)$ and integrating over the domain $s \in [-\tau, 0]$, we obtain the following:

$$\left(\int_{-\tau}^{0} \boldsymbol{\Psi}(s)\boldsymbol{\Psi}^{\mathrm{T}}(s)\,\mathrm{d}s\right)\dot{\boldsymbol{\beta}}(t) = \left(\int_{-\tau}^{0} \boldsymbol{\Psi}(s)\boldsymbol{\Psi}'(s)^{\mathrm{T}}\,\mathrm{d}s\right)\boldsymbol{\beta}(t) \tag{15}$$

Equation (15) can be rewritten as

$$\mathbf{C}\dot{\boldsymbol{\beta}}(t) = \mathbf{D}\boldsymbol{\beta}(t) \tag{16}$$

where $\mathbf{C}$ and $\mathbf{D}$ are square, block-diagonal matrices of dimension NP:

$$\mathbf{C} = \begin{bmatrix} \mathbf{C}^{(1)} & \mathbf{0} & \cdots & \mathbf{0} \\ \mathbf{0} & \mathbf{C}^{(2)} & \cdots & \mathbf{0} \\ \vdots & \vdots & \ddots & \vdots \\ \mathbf{0} & \mathbf{0} & \cdots & \mathbf{C}^{(P)} \end{bmatrix}^{\mathrm{T}} \tag{17a}$$

$$\mathbf{D} = \begin{bmatrix} \mathbf{D}^{(1)} & \mathbf{0} & \cdots & \mathbf{0} \\ \mathbf{0} & \mathbf{D}^{(2)} & \cdots & \mathbf{0} \\ \vdots & \vdots & \ddots & \vdots \\ \mathbf{0} & \mathbf{0} & \cdots & \mathbf{D}^{(P)} \end{bmatrix}^{\mathrm{T}} \tag{17b}$$

Submatrices $\mathbf{C}^{(i)}$ and $\mathbf{D}^{(i)}$ are defined as follows:

$$\mathbf{C}^{(i)} \triangleq \int_{-\tau}^{0} \phi_i(s)\phi_i^{\mathrm{T}}(s)\,\mathrm{d}s \tag{18a}$$

$$\mathbf{D}^{(i)} \triangleq \int_{-\tau}^{0} \phi_i(s)\phi_i'(s)^{\mathrm{T}}\,\mathrm{d}s \tag{18b}$$

Boundary conditions can be derived by substituting Eq. (13) into Eq. (9):

$$\boldsymbol{\Psi}^{\mathrm{T}}(0)\dot{\boldsymbol{\beta}}(t) = \left[-\mathbf{A}\boldsymbol{\Psi}^{\mathrm{T}}(0) - \sum_{q=1}^{m} \mathbf{B}_q\mathbf{K}_q^{\mathrm{T}}\boldsymbol{\Psi}^{\mathrm{T}}(-\tau_q)\right]\boldsymbol{\beta}(t) \tag{19}$$

Equations (16) and (19) can be combined as follows:

$$\mathbf{M}\dot{\boldsymbol{\beta}}(t) = \mathbf{K}\boldsymbol{\beta}(t) \tag{20}$$

Matrices $\mathbf{M}$ and $\mathbf{K}$ are of dimension $(NP + P) \times NP$ and are given by

$$\mathbf{M} \triangleq \begin{Bmatrix} \mathbf{C} \\ \bar{\mathbf{c}} \end{Bmatrix}, \qquad \mathbf{K} \triangleq \begin{Bmatrix} \mathbf{D} \\ \bar{\mathbf{d}} \end{Bmatrix} \tag{21}$$

where $\bar{\mathbf{c}}$ and $\bar{\mathbf{d}}$ are matrices of size $P \times NP$ containing the boundary conditions:

$$\bar{\mathbf{c}} \triangleq \mathbf{\Psi}^{\mathrm{T}}(0) \tag{22a}$$

$$\bar{\mathbf{d}} \triangleq -\mathbf{A}\mathbf{\Psi}^{\mathrm{T}}(0) - \sum_{q=1}^{m} \mathbf{B}_q \mathbf{K}_q^{\mathrm{T}} \mathbf{\Psi}^{\mathrm{T}}(-\tau_q) \tag{22b}$$

Equation (20) is an overdetermined system of $NP + P$ equations in NP unknowns; the least-squares solution can be computed as follows:

$$\dot{\boldsymbol{\beta}}(t) = \left(\mathbf{M}^{+}\mathbf{K}\right) \boldsymbol{\beta}(t) \tag{23}$$

where $\mathbf{M}^{+}$ is the Moore–Penrose inverse of $\mathbf{M}$. Finally, we define $\mathbf{G} \triangleq \mathbf{M}^{+}\mathbf{K}$ and write Eq. (23) as follows:

$$\dot{\boldsymbol{\beta}}(t) = \mathbf{G}\boldsymbol{\beta}(t) \tag{24}$$

Equation (24) is a system of ODEs that approximates the original system of DDEs (Eq. (3)). Consequently, the eigenvalues of $\mathbf{G}$ converge to the characteristic roots of Eq. (3) as the number of terms in the Galerkin approximation (N) increases [37]. Convergence can be monitored by substituting the computed eigenvalues of $\mathbf{G}$ into Eq. (4) (the characteristic equation of Eq. (3)) and calculating the absolute error (E). In this work, we consider eigenvalues to have converged when $E < 10^{-4}$. Also note that we use shifted Legendre polynomials as the basis functions:

$$\phi_1(s) = 1 \tag{25a}$$

$$\phi_2(s) = 1 + \tfrac{2s}{\tau} \tag{25b}$$

$$\phi_k(s) = \frac{(2k-3)\,\phi_2(s)\phi_{k-1}(s) - (k-2)\,\phi_{k-2}(s)}{k-1}, \quad k = 3, 4, \ldots, N \tag{25c}$$

Shifted Legendre polynomials have shown good convergence properties [37] and facilitate express-

ing the entries of matrices $\mathbf{C}^{(p)}$ and $\mathbf{D}^{(p)}$, as defined in Eq. (18), in closed form:

$$\mathbf{C}_{ij}^{(p)} = \begin{cases} \dfrac{\tau}{2i-1}, & \text{if } i = j \\ 0, & \text{otherwise} \end{cases} \tag{26a}$$

$$\mathbf{D}_{ij}^{(p)} = \begin{cases} 2, & \text{if } i < j \text{ and } i + j \text{ is odd} \\ 0, & \text{otherwise} \end{cases} \tag{26b}$$

where $i = 1, 2, \ldots, N$; $j = 1, 2, \ldots, N$; and $\tau = \max(\tau_1, \tau_2, \ldots, \tau_m)$.

3 Verification of Pseudoinverse Method

In this section, we verify the pseudoinverse-based Galerkin approximation method by applying the procedure described in Section 2.2 to two test problems. We compare our results to those obtained using the Quasi-Polynomial mapping-based Root-finder (QPmR) algorithm [40] and the pseudospectral differencing (PSD) method [29, 41].

3.1 First-order DDE with two delays

Consider the following first-order DDE with delays τ and $\tau + b$:

$$\dot{x}(t) = ax(t) + \frac{x(t-\tau) - x(t-\tau-b)}{b} \tag{27}$$

The characteristic equation is obtained by substituting $x(t) = e^{st}$:

$$s - a - \tfrac{1}{b}e^{-s\tau} + \tfrac{1}{b}e^{-s(\tau+b)} = 0 \tag{28}$$

To test the robustness of the proposed approach, we find the rightmost roots of Eq. (28) using parameters $\tau = 1$ and $a = b = 10^r$ for $r = -1, -2, \ldots, -6$. As shown in Figures 1 and 2,

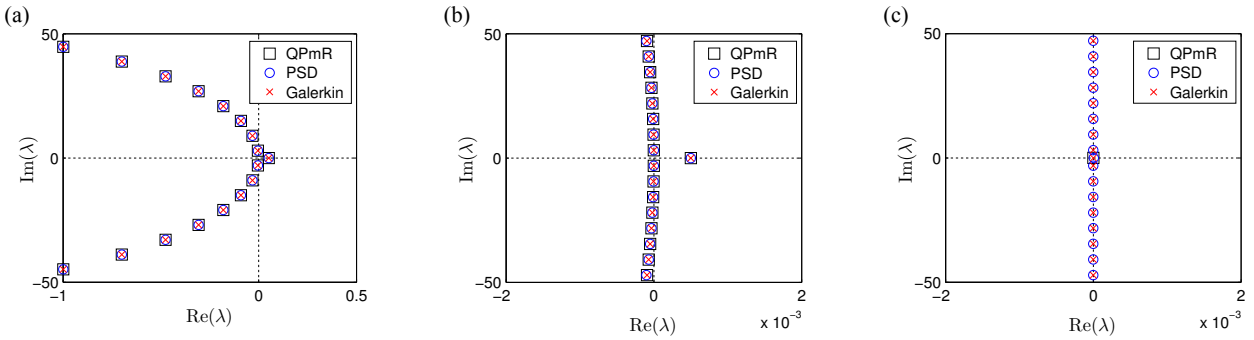

Figure 1: Characteristic roots of Eq. (27) using the Quasi-Polynomial mapping-based Root-finder (QPmR) algorithm, the pseudospectral differencing (PSD) method, and the proposed pseudoinverse-based Galerkin approximation method: (a) $a = b = 10^{-1}$, (b) $a = b = 10^{-3}$, and (c) $a = b = 10^{-6}$.

the roots obtained using the pseudoinverse-based Galerkin approach compare favorably with those obtained using the existing QPmR [40] and PSD [29, 41] methods. As expected from inspection of Eq. (28), the rightmost root approaches zero as r decreases. The three methods have very similar precision; for example, when $a = b = 10^{-6}$, the errors are $E_{\text{Galerkin}} = 1.000124 \times 10^{-6}$, $E_{\text{PSD}} = 1.000008 \times 10^{-6}$, and $E_{\text{QPmR}} = 0.999891 \times 10^{-6}$. However, note in Figure 1(c) that the QPmR method identified only one root when $a = b = 10^{-6}$. Another disadvantage of the QPmR method is the requirement to specify the region of the complex plane into which the poles should be placed.

Based on the results of Figure 1, the pseudospectral differencing method appears to perform well. The proposed pseudoinverse-based Galerkin approximation method was further compared with the PSD method using a Monte Carlo simulation. We computed the roots of Eq. (28) using $N = 25k$ for $k = 1, 2, \ldots, 5$, where N is the size of the linear eigenvalue problem being solved.

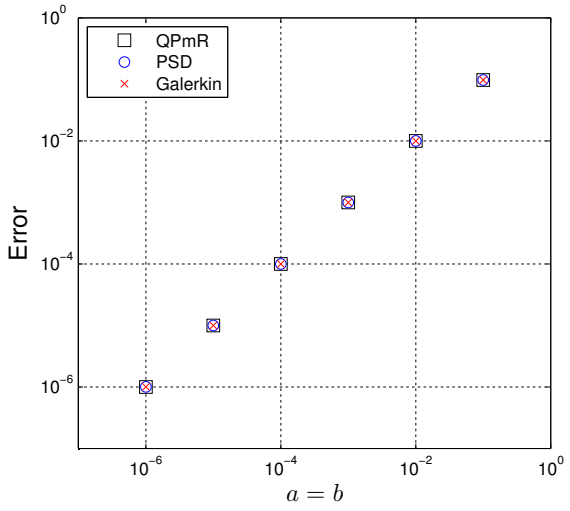

Figure 2: Errors obtained upon substituting into the characteristic equation (Eq. (28)) the rightmost eigenvalue computed using the Quasi-Polynomial mapping-based Root-finder (QPmR) algorithm, the pseudospectral differencing (PSD) method, and the proposed pseudoinverse-based Galerkin approximation method.

Table 1: Number of converged roots of Eq. (28), averaged over 10,000 trials.

N	Galerkin method	PSD method
25	8.0	6.0
50	21.5	15.4
75	34.4	25.8
100	48.5	36.3
125	63.2	48.0

In the Galerkin method, N corresponds to the number of terms in the series solution (Eq. (11)); in the PSD method, N is the number of collocation points. We selected parameters uniformly from the ranges $a \in [1, 10]$, $b \in [1, 5]$, and $\tau \in [0.1, 5.1]$, repeating 10,000 times for each value of N. On average, more roots converged using the proposed Galerkin method than the PSD method, as shown in Table 1.

3.2 Second-order DDE with three delays

Consider the following second-order DDE with delays τ_1, τ_2, and $\tau_1 + \tau_2$:

$$\ddot{x}(t) + a_1\dot{x}(t) + a_2x(t) + a_3\dot{x}(t-\tau_1) + a_4x(t-\tau_1) + a_5\dot{x}(t-\tau_2) + a_6\dot{x}(t-\tau_1-\tau_2) = 0 \tag{29}$$

where $a_1 = 7.1$, $a_2 = 21.1425$, $a_3 = 6$, $a_4 = 14.8$, $a_5 = 2$, and $a_6 = 8$. As demonstrated by the stability chart shown in Figure 3, the results obtained using the proposed Galerkin method are in agreement with those obtained using the spectral tau method [24, 37].

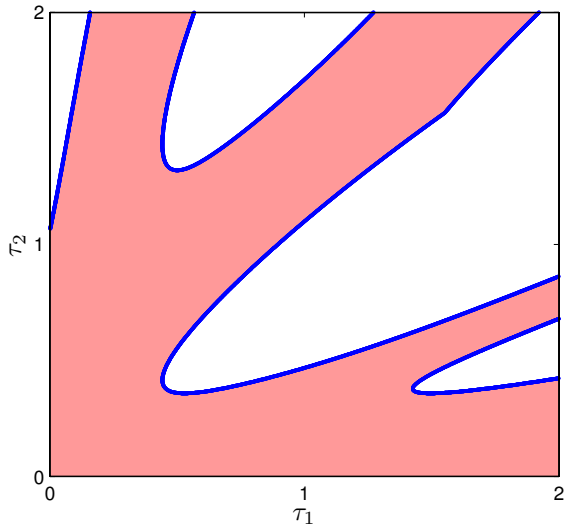

Figure 3: Stability diagram for the second-order DDE given by Eq. (29) obtained using the spectral tau method (red region) and the proposed pseudoinverse-based Galerkin approximation method (blue lines).

4 Results and Discussion

In this section, we apply the methods described in Section 2 to two example problems taken from the literature [11, 14]. We obtain the characteristic roots of DDEs using the pseudoinverse-based Galerkin approximation method and improve closed-loop stability using the proposed optimization strategy.

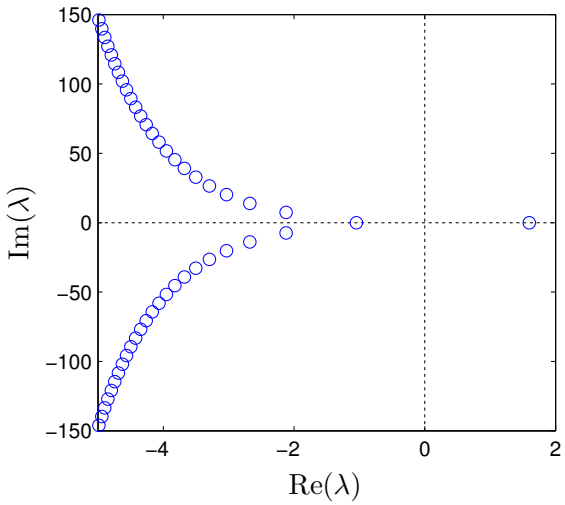

Figure 4: Rightmost characteristic roots of Eq. (30) using initial feedback gain $k = 0.8$.

4.1 Example from Niu et al.

Consider the following first-order system [14]:

$$\dot{x}(t) = ax(t) + a_d x(t - \tau) + u(t) \tag{30a}$$

$$u(t) = kx(t) \tag{30b}$$

where $a = \tau = 1$ and $a_d = -1$. We use $N = 100$ terms in the series solution (Eq. (11)), thereby converting Eq. (30) into a system of ODEs of the form given by Eq. (24), where $\mathbf{G} \in \mathbb{R}^{100\times 100}$. We select an initial guess of $k = 0.8$, which results in the rightmost eigenvalues shown in Figure 4. Note that the rightmost eigenvalue has a positive real component ($\mathrm{Re}\,(\lambda_{\max}) = 1.5976$). Thus, the system is unstable for $k = 0.8$.

To stabilize this system, we set $\alpha = 1$ in the objective function (Eq. (2)) and solve the minimization problem using the Nelder–Mead algorithm in MATLAB via the `fminsearch` function. The optimal gain was found to be $k^* = -3.5978$, resulting in the rightmost eigenvalues shown in

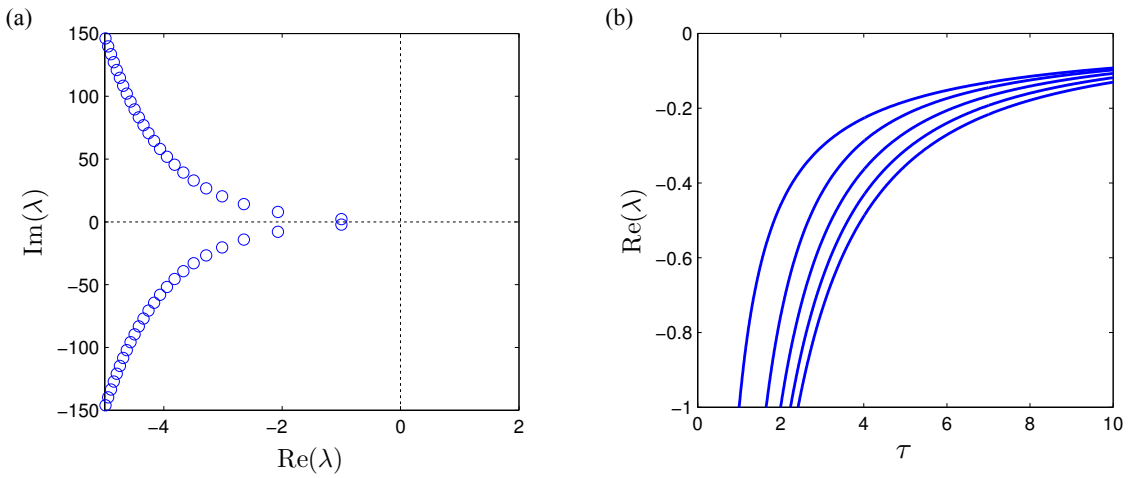

Figure 5: Rightmost characteristic roots of Eq. (30) with delay $\tau = 1$ (a) and the variation of the five rightmost roots with respect to delay τ (b) using optimal feedback gain $k^* = -3.5978$.

Figure 5(a). Note that the rightmost eigenvalue has a real component of -1, indicating that stability has been achieved. As shown in Figure 5(b), the system will remain stable for delays substantially greater than $\tau = 1$ when using feedback gain k^*. Note that the optimal objective function value of $J^* = 0$ is obtained when $\alpha = 1$ in the objective function (Eq. (2)), indicating that α could be increased to achieve an even larger stability margin.

4.2 Example from Michiels et al.

We now consider the following third-order system [11]:

$$\dot{\mathbf{x}}(t) = \mathbf{A}\mathbf{x}(t) + \mathbf{B}\mathbf{u}(t-\tau) \tag{31a}$$

$$\mathbf{u}(t) = \mathbf{K}^{\mathrm{T}}\mathbf{x}(t) \tag{31b}$$

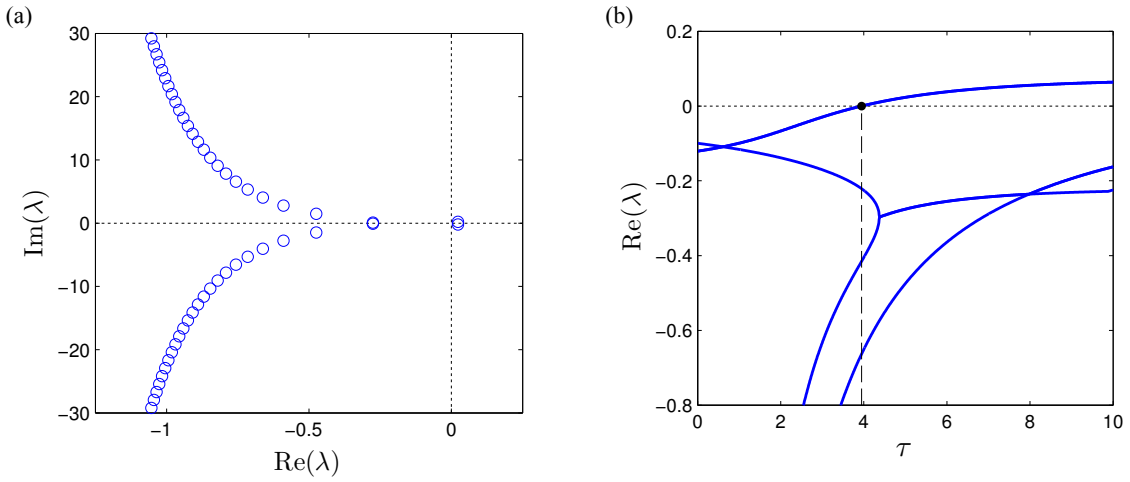

Figure 6: Rightmost characteristic roots of Eq. (31) with delay $\tau = 5$ (a) and the variation of the rightmost roots with respect to delay τ (b) using initial feedback gains $\mathbf{K} = [0.719, 1.04, 1.29]^{\mathrm{T}}$.

where delay $\tau = 5$, and $\mathbf{A}$ and $\mathbf{B}$ are defined as follows:

$$\mathbf{A} = \begin{bmatrix} -0.08 & -0.03 & 0.2 \\ 0.2 & -0.04 & -0.005 \\ -0.06 & 0.2 & -0.07 \end{bmatrix}, \qquad \mathbf{B} = \begin{Bmatrix} -0.1 \\ -0.2 \\ 0.1 \end{Bmatrix} \tag{32}$$

We again use $N = 100$ terms in the series solution (Eq. (11)), now obtaining a system of ODEs (Eq. (24)) in which $\mathbf{G} \in \mathbb{R}^{300\times300}$. We use as an initial guess the gains reported in Michiels et al. [11]: $\mathbf{K} = [0.719, 1.04, 1.29]^{\mathrm{T}}$. As shown in Figure 6, the rightmost eigenvalues have a positive real component when the delay is $\tau = 5$ ($\mathrm{Re}\,(\lambda_{\max}) = 0.0232$) and the system is stable only for delays $\tau < 3.9466$.

The system can be stabilized using the same procedure as before. We set $\alpha = 1$ in the objective function (Eq. (2)) and minimize using the Nelder–Mead algorithm. The optimal gains were found to be $\mathbf{K}^* = [0.5473, 0.8681, 0.5998]^{\mathrm{T}}$; as shown in Figure 7(a), the rightmost eigenvalue

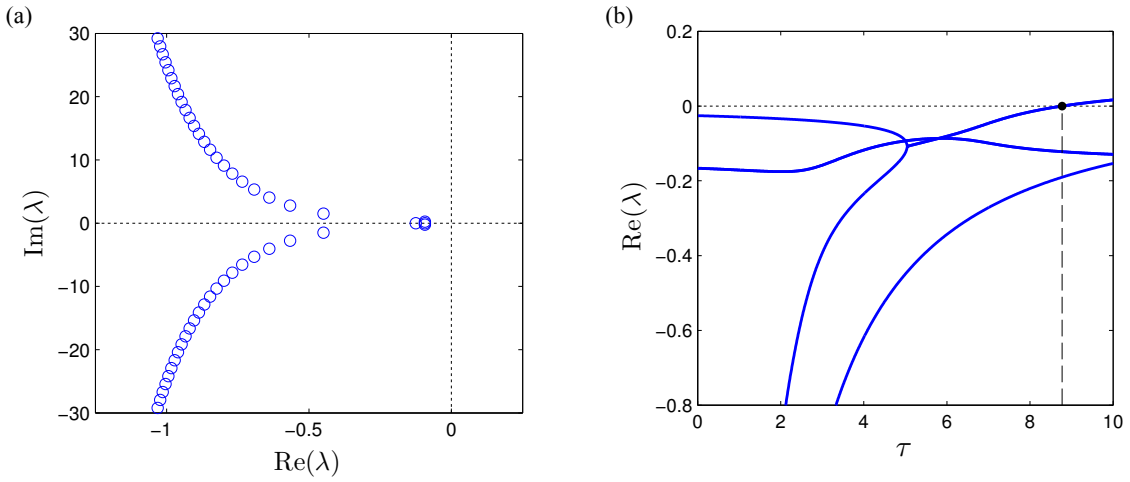

Figure 7: Rightmost characteristic roots of Eq. (31) with delay $\tau = 5$ (a) and the variation of the rightmost roots with respect to delay τ (b) using optimal feedback gains $\mathbf{K}^* = [0.5473, 0.8681, 0.5998]^{\mathrm{T}}$.

was moved to $\mathrm{Re}\,(\lambda_{\max}) = -0.0931$. Once again, the rightmost eigenvalue has a negative real component and, thus, the closed-loop system is stable. As shown in Figure 7(b), the system will remain stable for delays up to $\tau = 8.7739$ using optimal feedback gains $\mathbf{K}^*$. In contrast to the example of Section 4.1, the optimal objective function value is greater than zero ($J^* = 0.8223$) in this case, indicating that the stability margin cannot be increased by increasing α.

5 Experimental Validation

In this section, we validate the proposed Galerkin method using the rotary inverted pendulum apparatus (QUBE-Servo Rotary Servo Experiment, Quanser Inc., Markham, Ontario, Canada) shown in Figure 8. The apparatus consists of a free-swinging rigid pendulum mounted to the end of a servo-driven rotary arm. The position of the arm is given by θ as it rotates about the vertical axis;

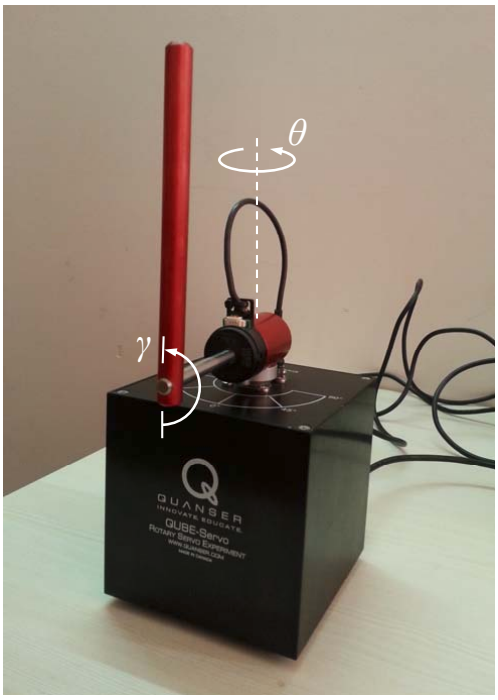

Figure 8: Rotary inverted pendulum apparatus, shown here with $\theta \approx 0°$ and $\gamma \approx 180°$.

the position of the pendulum is $\gamma = 0^\circ$ when hanging at rest and $\gamma = 180^\circ$ when inverted.

The linearized equations of motion for the rotary inverted pendulum system are as follows:

$$\left(J_r + m_p \ell_r^2\right) \ddot{\theta}(t) - \tfrac{1}{2} m_p \ell_p \ell_r \ddot{\gamma}(t) = T(t) - B_r \dot{\theta}(t) \tag{33a}$$

$$\left(J_p + \tfrac{1}{4} m_p \ell_p^2\right) \ddot{\gamma}(t) - \tfrac{1}{2} m_p \ell_p \ell_r \ddot{\theta}(t) - \tfrac{1}{2} m_p \ell_p g \gamma(t) = -B_p \dot{\gamma}(t) \tag{33b}$$

where ℓ_p, m_p, and J_p are the pendulum's length, mass, and moment of inertia with respect to its pivot; ℓ_r is the length of the rotary arm; J_r is the equivalent moment of inertia acting on the servo shaft; B_p and B_r represent the viscous damping about the pendulum's pivot and the servo shaft, respectively; g is the gravitational acceleration; and $T(t)$ is the torque applied to the rotary arm by the servo. The torque $T(t)$ can be computed as follows:

$$T(t) = \frac{k_m}{R_m} \left(V_m(t) - \frac{k_m^2}{R_m} \dot{\theta}(t) \right) \tag{34}$$

where k_m is the DC motor back-emf constant, R_m is the electrical resistance of the DC motor armature, and $V_m(t)$ is the control input (voltage). The numerical values of these parameters are provided by Quanser [42] and are listed in Table 2. The linearized equations of motion for the rotary inverted pendulum system (Eq. (33)) can be expressed in state-space form:

$$\dot{\mathbf{x}}(t) = \mathbf{A}\mathbf{x}(t) + \mathbf{B}u(t) \tag{35a}$$

$$u(t) = -\mathbf{K}^{\mathrm{T}}\mathbf{x}(t) \tag{35b}$$

where $\mathbf{x} \triangleq \left[\theta(t), \gamma(t), \dot{\theta}(t), \dot{\gamma}(t)\right]^{\mathrm{T}}$, $u(t) \triangleq V(t)$, and $\mathbf{A}$ and $\mathbf{B}$ are given as follows:

$$\mathbf{A} = \begin{bmatrix} 0 & 0 & 1 & 0 \\ 0 & 0 & 0 & 1 \\ 0 & 149.2751 & -0.0104 & 0 \\ 0 & 261.6091 & -0.0103 & 0 \end{bmatrix}, \qquad \mathbf{B} = \begin{Bmatrix} 0 \\ 0 \\ 49.7275 \\ 49.1493 \end{Bmatrix} \tag{36}$$

Table 2: Parameter values for the rotary inverted pendulum apparatus [42].

Parameter	Value	Units
ℓ_p	0.129	m
ℓ_r	0.085	m
m_p	0.024	kg
J_p	3.32820×10^{-5}	kg m^2
J_r	5.71979×10^{-5}	kg m^2
B_p	0	N m s/rad
B_r	0	N m s/rad
R_m	8.4	Ω
k_m	0.042	V s/rad
g	9.81	m/s^2

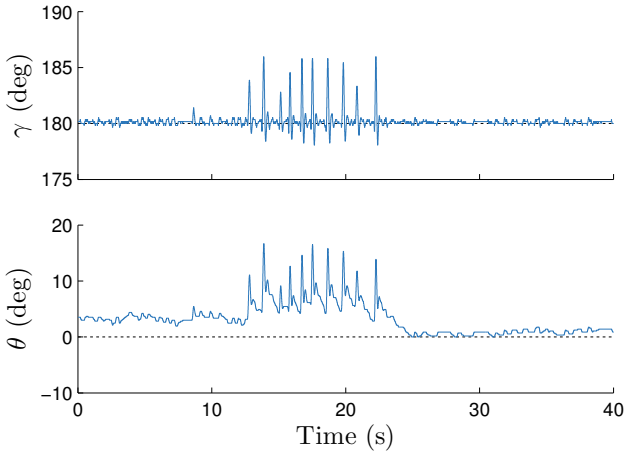

Figure 9: Stable response of the inverted pendulum (γ) and rotary arm (θ) with inherent delay of 2 ms and feedback gains $\mathbf{K} = [-2, 30, -2, 2.5]^{\mathrm{T}}$. An external disturbance is applied between 13 and 23 seconds.

The controller samples at a rate of 500 Hz; thus, the system has an inherent delay of 2 ms. We begin by controlling the rotary inverted pendulum system without introducing any additional delays. We use feedback gains $\mathbf{K} = [-2, 30, -2, 2.5]^{\mathrm{T}}$, which are provided by Quanser for the balance control exercise [43]. The steady-state response of the physical system is shown in Figure 9. The system is stable about its vertical equilibrium ($\gamma = 180°$) and recovers from an external disturbance.

We now introduce an additional sensing delay τ, resulting in the following state-space representation of the rotary inverted pendulum system:

$$\dot{\mathbf{x}}(t) = \mathbf{A}\mathbf{x}(t) + \mathbf{B}u(t - \tau) \tag{37}$$

where $\mathbf{A}$ and $\mathbf{B}$ are given by Eq. (36). We first assess the stability of the system using the proposed pseudoinverse-based Galerkin method, then verify our predictions experimentally. The real

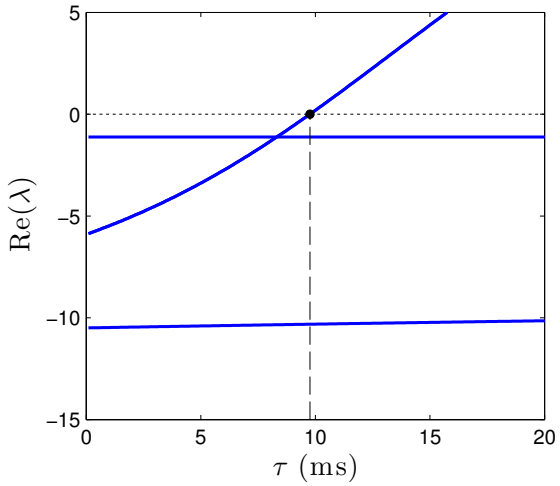

Figure 10: Variation of the rightmost roots of Eq. (37) with respect to delay τ using feedback gains $\mathbf{K} = [-2, 30, -2, 2.5]^{\mathrm{T}}$. The critical delay is $\tau = 9.76$ ms.

component of the rightmost roots of the system are shown in Figure 10 as functions of delay τ, using the same feedback gains $\mathbf{K}$ as above. The *critical delay* is the delay at which the system will become unstable; as shown, the simulations indicate a critical delay of $\tau = 9.76$ ms. As shown in Figure 11, the four rightmost characteristic roots of Eq. (37) lie in the left half of the complex plane when $\tau = 5$ ms, indicating that the system is stable; when $\tau = 10$ ms, two roots are in the right half of the complex plane and the system is unstable.

We validate experimentally by deliberately introducing additional delay into the feedback controller, in increments of 0.5 ms. The physical system remained stable when delays of up to 7.5 ms were introduced (Figure 12) and was unstable with an additional delay of 8 ms (Figure 13). Thus, when added to the inherent delay of 2 ms, the physical system exhibited a critical delay of between 9.5 and 10 ms, which is in agreement with the predicted critical delay of $\tau = 9.76$ ms.

We now stabilize Eq. (37) with delay $\tau = 10$ ms using the pseudoinverse-based Galerkin

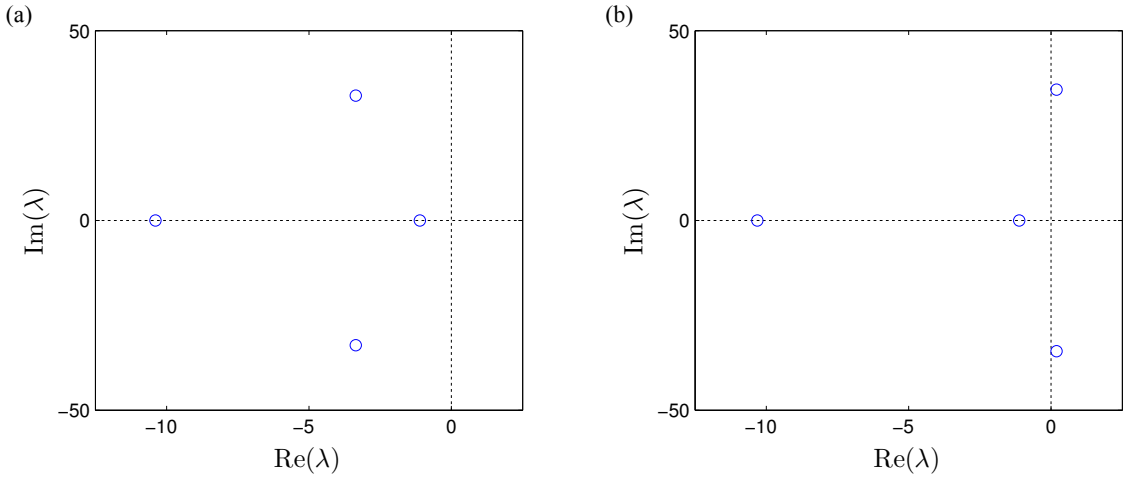

Figure 11: Rightmost characteristic roots of Eq. (37) with delay (a) $\tau = 5$ ms and (b) $\tau = 10$ ms, using feedback gains $\mathbf{K} = [-2, 30, -2, 2.5]^{\mathrm{T}}$.

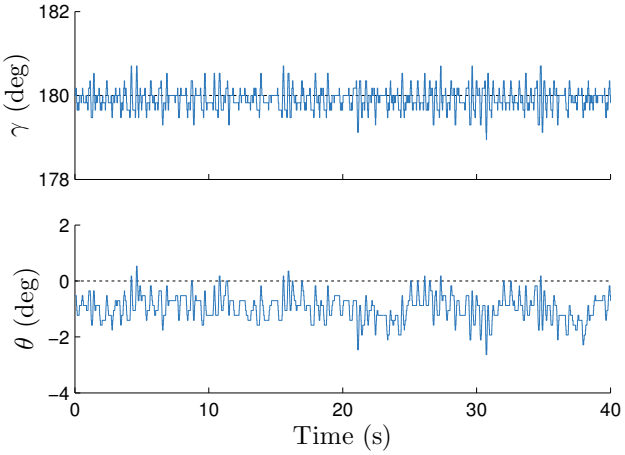

Figure 12: Stable response of the inverted pendulum (γ) and rotary arm (θ) with total delay of $\tau = 2 + 7.5 = 9.5$ ms and feedback gains $\mathbf{K} = [-2, 30, -2, 2.5]^{\mathrm{T}}$.

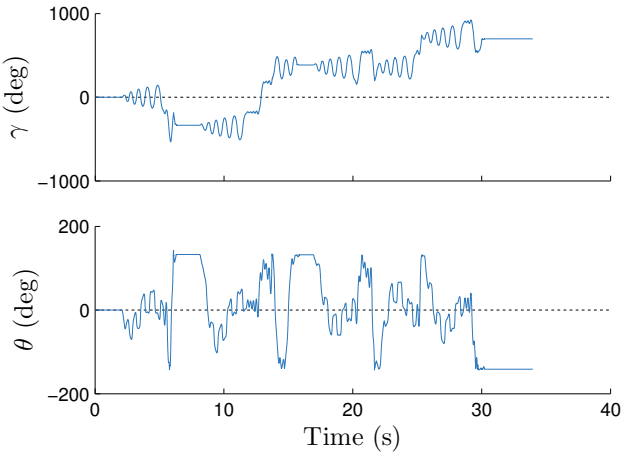

Figure 13: Unstable response of the inverted pendulum (γ) and rotary arm (θ) with total delay of $\tau = 2 + 8 = 10$ ms and feedback gains $\mathbf{K} = [-2, 30, -2, 2.5]^{\mathrm{T}}$.

method and the procedure described in Section 2. We set $\alpha = \alpha_0 = 1$ in the objective function (Eq. (2)) and solve the minimization problem using the Nelder–Mead algorithm in MATLAB via the `fminsearch` function. We repeat the optimization procedure, increasing α by $\delta\alpha = 1$ each iteration, until the real component of the rightmost pole is unable to reach $-\alpha$. In this case, the algorithm terminates at $\alpha = 6$, where the objective function value is $J^* = 0.000222$, the optimal feedback gains are $\mathbf{K}^* = [-2.3443, 31.3406, -1.1797, 2.7717]^{\mathrm{T}}$, and the rightmost pole location is $\mathrm{Re}\,(\lambda_{\max}) = -5.9851$. As shown in Figure 14, the physical system is stable when a delay of 10 ms is introduced deliberately (producing a total delay of $\tau = 12$ ms) and recovers from an external disturbance. As shown, the system is robust to external disturbances even without controlling the frequency of oscillations induced by the optimal feedback gains.

The pseudoinverse-based Galerkin method predicts a critical delay of $\tau = 17.7$ ms when using the optimal feedback gains $\mathbf{K}^*$ computed above (Figure 15). We again validate this result exper-

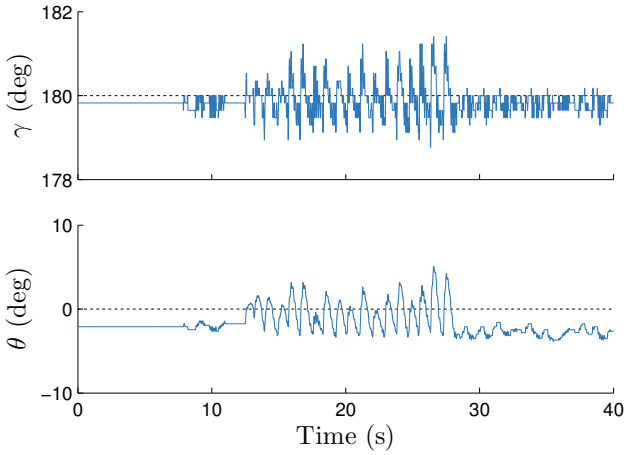

Figure 14: Stable response of the inverted pendulum (γ) and rotary arm (θ) with total delay of $\tau = 2 + 10 = 12$ ms and optimal feedback gains $\mathbf{K}^* = [-2.3443, 31.3406, -1.1797, 2.7717]^{\mathrm{T}}$. An external disturbance is applied between 12 and 27 seconds.

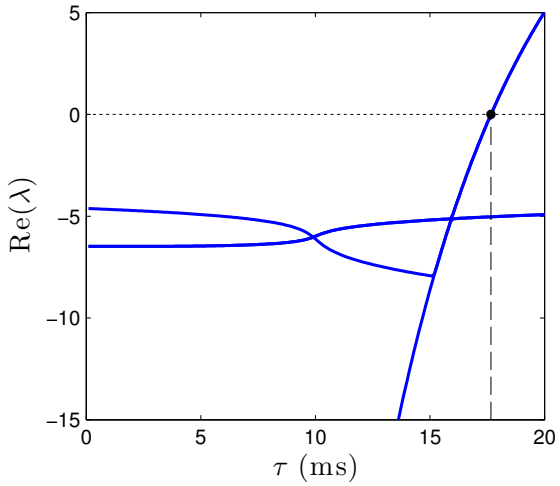

Figure 15: Variation of the rightmost roots of Eq. (37) with respect to delay τ using optimal feedback gains $\mathbf{K}^* = [-2.3443, 31.3406, -1.1797, 2.7717]^{\mathrm{T}}$. The critical delay is $\tau = 17.7$ ms.

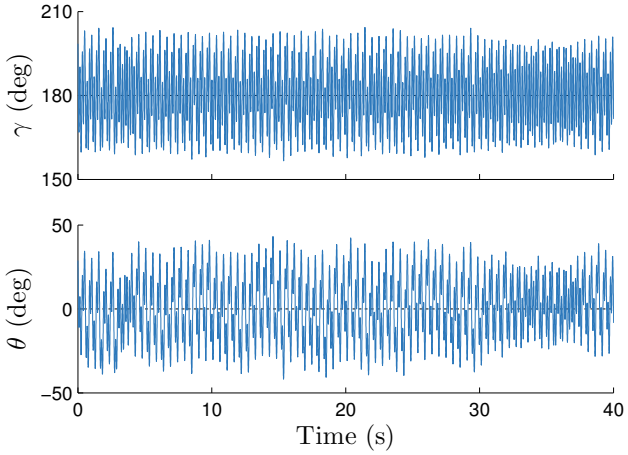

Figure 16: Stable response of the inverted pendulum (γ) and rotary arm (θ) with total delay of $\tau = 2 + 15 = 17$ ms and optimal feedback gains $\mathbf{K}^* = [-2.3443, 31.3406, -1.1797, 2.7717]^{\mathrm{T}}$.

imentally by deliberately introducing additional delay into the feedback controller, in increments of 0.5 ms. The physical system remained stable when delays of up to 15 ms were introduced (Figure 16) and was unstable when this delay was increased to 15.5 ms (Figure 17). Thus, when added to the inherent delay of 2 ms, the physical system exhibited a critical delay of between 17 and 17.5 ms, which is within 1–4% of the predicted critical delay of $\tau = 17.7$ ms. The pseudoinverse-based Galerkin method provided a simple and reliable means of predicting and optimizing the stability of the rotary inverted pendulum system.

6 Conclusions

In this work, we have explored the pole placement problem for time-delayed systems. We have developed a Galerkin approximation method using a new pseudoinverse-based strategy for embedding the boundary conditions, and have verified our results through comparison to those obtained

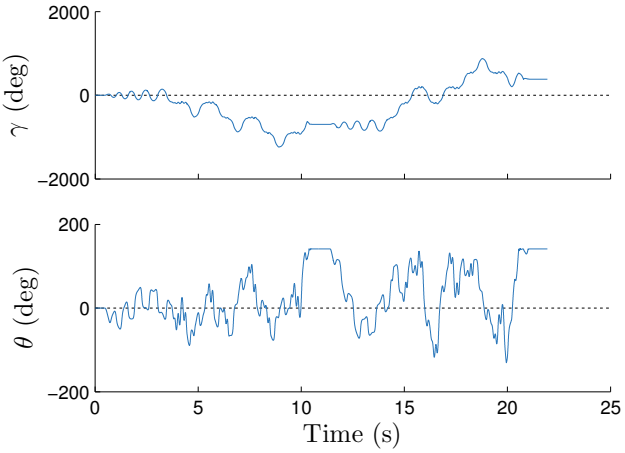

Figure 17: Unstable response of the inverted pendulum (γ) and rotary arm (θ) with total delay of $\tau = 2 + 15.5 = 17.5$ ms and optimal feedback gains $\mathbf{K}^* = [-2.3443, 31.3406, -1.1797, 2.7717]^{\mathrm{T}}$.

using the Quasi-Polynomial mapping-based Root-finder algorithm, the pseudospectral differencing method, and the spectral tau method. The proposed Galerkin method results in a simpler mathematical derivation than we have presented previously. We validated our method experimentally by stabilizing a rotary inverted pendulum system with inherent and deliberate state feedback delays. A simple optimization strategy was employed to increase the time-delay stability margin.

Unlike many existing techniques, the proposed approach can be readily extended to systems in which the coefficients and/or delays are time-periodic. Although we used a simple algorithm to solve the pole placement problem in this work, a more sophisticated optimization problem could be formulated to include other considerations. For example, unilateral constraints could be introduced to limit the maximum value of the controller gains, or terms could be added to the objective function to balance increasing the stability margin with minimizing the control effort.

Acknowledgements

C.P.V. gratefully acknowledges the Department of Science and Technology for funding this research through the Inspire fellowship (DST/INSPIRE/04/2014/000972). We thank Dr. K. Detroja for providing the equipment used in Section 5. S.S.K. thanks S. Subhash for his assistance performing the experiments.

References

[1] Richard, J.-P., 2003. "Time-delay systems: an overview of some recent advances and open problems". *Automatica,* **39**(10), pp. 1667–1694.

[2] Balachandran, B., 2001. "Nonlinear dynamics of milling processes". *Philosophical Transactions of the Royal Society A: Mathematical, Physical and Engineering Sciences,* **359**(1781), pp. 793–819.

[3] VanWiggeren, G. D., and Roy, R., 1998. "Communication with chaotic lasers". *Science,* **279**(5354), pp. 1198–1200.

[4] Nise, N. S., 2000. *Control Systems Engineering*, 3rd ed. John Wiley & Sons, New York, NY, U.S.A.

[5] Insperger, T., and Stépán, G., 2007. "Act-and-wait control concept for discrete-time systems with feedback delay". *IET Control Theory & Applications,* **1**(3), pp. 553–557.

[6] Yi, S., Nelson, P. W., and Ulsoy, A. G., 2010. *Time-Delay Systems: Analysis and Control Using the Lambert W Function*. World Scientific, Hackensack, NJ, U.S.A.

[7] Yi, S., Nelson, P. W., and Ulsoy, A. G., 2010. "Eigenvalue assignment via the Lambert W function for control of time-delay systems". *Journal of Vibration and Control,* **16**(7–8), pp. 961–982.

[8] Lavaei, J., Sojoudi, S., and Murray, R. M., 2010. "Simple delay-based implementation of continuous-time controllers". In Proceedings of the 2010 American Control Conference, Baltimore, MD, U.S.A., June 30–July 2, pp. 5781–5788.

[9] Orosz, G., Moehlis, J., and Murray, R. M., 2010. "Controlling biological networks by time-delayed signals". *Philosophical Transactions of the Royal Society A: Mathematical, Physical and Engineering Sciences,* **368**(1911), pp. 439–454.

[10] Bekiaris-Liberis, N., Jankovic, M., and Krstic, M., 2013. "Adaptive stabilization of LTI systems with distributed input delay". *International Journal of Adaptive Control and Signal Processing,* **27**(1–2), pp. 46–65.

[11] Michiels, W., Engelborghs, K., Vansevenant, P., and Roose, D., 2002. "Continuous pole placement for delay equations". *Automatica,* **38**(5), pp. 747–761.

[12] Michiels, W., Vyhlídal, T., and Zítek, P., 2010. "Control design for time-delay systems based on quasi-direct pole placement". *Journal of Process Control,* **20**(3), pp. 337–343.

[13] Vyhlídal, T., Michiels, W., and McGahan, P., 2010. "Synthesis of strongly stable state-derivative controllers for a time-delay system using constrained non-smooth optimization". *IMA Journal of Mathematical Control and Information,* **27**(4), pp. 437–455.

[14] Niu, J., Ding, Y., Zhu, L., and Ding, H., 2015. "Eigenvalue assignment for control of time-delay systems via the generalized Runge–Kutta method". *Journal of Dynamic Systems, Measurement, and Control,* **137**(9), p. 091003.

[15] Burke, J. V., Lewis, A. S., and Overton, M. L., 2005. "A robust gradient sampling algorithm for nonsmooth, nonconvex optimization". *SIAM Journal on Optimization,* **15**(3), pp. 751–779.

[16] Vanbiervliet, J., Verheyden, K., Michiels, W., and Vandewalle, S., 2008. "A nonsmooth optimisation approach for the stabilisation of time-delay systems". *ESAIM: Control, Optimisation and Calculus of Variations,* **14**(3), pp. 478–493.

[17] Yi, S., Nelson, P. W., and Ulsoy, A. G., 2013. "Proportional-integral control of first-order time-delay systems via eigenvalue assignment". *IEEE Transactions on Control Systems Technology,* **21**(5), pp. 1586–1594.

[18] Wei, F., Bachrathy, D., Orosz, G., and Ulsoy, A. G., 2014. "Spectrum design using distributed delay". *International Journal of Dynamics and Control,* **2**(2), pp. 234–246.

[19] Asl, F. M., and Ulsoy, A. G., 2003. "Analysis of a system of linear delay differential equations". *Journal of Dynamic Systems, Measurement, and Control,* **125**(2), pp. 215–223.

[20] Jarlebring, E., and Damm, T., 2007. "The Lambert W function and the spectrum of some multidimensional time-delay systems". *Automatica,* **43**(12), pp. 2124–2128.

[21] Yi, S., Nelson, P. W., and Ulsoy, A. G., 2007. "Survey on analysis of time delayed systems via the Lambert W function". *Dynamics of Continuous, Discrete and Impulsive Systems, Series A: Mathematical Analysis,* **14**(S2), pp. 296–301.

[22] Wahi, P., and Chatterjee, A., 2005. "Asymptotics for the characteristic roots of delayed dynamic systems". *Journal of Applied Mechanics,* **72**(4), pp. 475–483.

[23] Vyasarayani, C. P., 2012. "Galerkin approximations for higher order delay differential equations". *Journal of Computational and Nonlinear Dynamics,* **7**(3), p. 031004.

[24] Sadath, A., and Vyasarayani, C. P., 2015. "Galerkin approximations for stability of delay differential equations with distributed delays". *Journal of Computational and Nonlinear Dynamics,* **10**(6), p. 061024.

[25] Kalmár-Nagy, T., 2009. "Stability analysis of delay-differential equations by the method of steps and inverse Laplace transform". *Differential Equations and Dynamical Systems,* **17**(1–2), pp. 185–200.

[26] Insperger, T., and Stépán, G., 2011. *Semi-Discretization for Time-Delay Systems: Stability and Engineering Applications*. Springer, New York, NY, U.S.A.

[27] Wahi, P., and Chatterjee, A., 2005. "Galerkin projections for delay differential equations". *Journal of Dynamic Systems, Measurement, and Control,* **127**(1), pp. 80–87.

[28] Butcher, E. A., Ma, H., Bueler, E., Averina, V., and Szabo, Z., 2004. "Stability of linear time-periodic delay-differential equations via Chebyshev polynomials". *International Journal for Numerical Methods in Engineering,* **59**(7), pp. 895–922.

[29] Breda, D., Maset, S., and Vermiglio, R., 2005. "Pseudospectral differencing methods for characteristic roots of delay differential equations". *SIAM Journal on Scientific Computing,* **27**(2), pp. 482–495.

[30] Wu, Z., and Michiels, W., 2012. "Reliably computing all characteristic roots of delay differential equations in a given right half plane using a spectral method". *Journal of Computational and Applied Mathematics,* **236**(9), pp. 2499–2514.

[31] Mann, B. P., and Patel, B. R., 2010. "Stability of delay equations written as state space models". *Journal of Vibration and Control,* **16**(7–8), pp. 1067–1085.

[32] Khasawneh, F. A., and Mann, B. P., 2011. "A spectral element approach for the stability of delay systems". *International Journal for Numerical Methods in Engineering,* **87**(6), pp. 566–592.

[33] Sun, J.-Q., 2009. "A method of continuous time approximation of delayed dynamical systems". *Communications in Nonlinear Science and Numerical Simulation,* **14**(4), pp. 998–1007.

[34] Song, B., and Sun, J.-Q., 2011. "Lowpass filter-based continuous-time approximation of delayed dynamical systems". *Journal of Vibration and Control,* **17**(8), pp. 1173–1183.

[35] Koto, T., 2004. "Method of lines approximations of delay differential equations". *Computers & Mathematics with Applications,* **48**(1–2), pp. 45–59.

[36] Engelborghs, K., and Roose, D., 2002. "On stability of LMS methods and characteristic roots of delay differential equations". *SIAM Journal on Numerical Analysis,* **40**(2), pp. 629–650.

[37] Vyasarayani, C. P., Subhash, S., and Kalmár-Nagy, T., 2014. "Spectral approximations for characteristic roots of delay differential equations". *International Journal of Dynamics and Control,* **2**(2), pp. 126–132.

[38] Sadath, A., and Vyasarayani, C. P., 2015. "Galerkin approximations for stability of delay differential equations with time periodic coefficients". *Journal of Computational and Nonlinear Dynamics,* **10**(2), p. 021011.

[39] Sadath, A., and Vyasarayani, C. P., 2015. "Galerkin approximations for stability of delay differential equations with time periodic delays". *Journal of Computational and Nonlinear Dynamics,* **10**(6), p. 061008.

[40] Vyhlídal, T., and Zítek, P., 2014. "QPmR - Quasi-Polynomial Root-finder: algorithm update and examples". In *Delay Systems: From Theory to Numerics and Applications. Advances in Delays and Dynamics, vol. 1*, T. Vyhlídal, J.-F. Lafay, and R. Sipahi, eds. Springer, Cham, Switzerland.

[41] Breda, D., Maset, S., and Vermiglio, R., 2015. *Stability of Linear Delay Differential Equations: A Numerical Approach with MATLAB*. Springer, New York, NY, U.S.A.

[42] Apkarian, J., Lévis, M., and Martin, P., 2016. Instructor Workbook: QUBE-Servo 2 Experiment for MATLAB/Simulink Users. Tech. rep. Quanser Inc., Markham, ON, Canada, Report No. v 1.0.

[43] Apkarian, J., Karam, P., and Lévis, M., 2012. Student Workbook: Inverted Pendulum Experiment for LabVIEW Users. Tech. rep. Quanser Inc., Markham, ON, Canada, Report No. v 1.1.